Supporting information

Defective Two-dimensional Layered Heterometallic Phosphonate as Highly Efficient Oxygen Evolution Electrocatalyst

Chong-Chong Yan, Si-Fu Tang*
College of Chemistry and Pharmaceutical Sciences, Qingdao Agricultural University, Changcheng Road 700, Chengyang District, Qingdao 266109, China.

Materials and Instruments.

The ligand (((1,3,5-triazine-2,4,6-triyl)tris(benzene-4,1-diyl))tris(methylene))tris (phosphonic acid) (H_6L) was synthesized according to literature [1]. Powder X-ray diffraction patterns (see Figure S2) were obtained on a Bruker D8 Advance diffractometer using CuKα radiation. IR spectra were recorded in the range of 4000-400 cm^{-1} on a Thermo Fisher Nicolet iS-5 FTIR Spectrometer with KBr pellets. Thermogravimetric analyses (TGA) of QAU-1-Ni-C and QAU-1-Co-C were performed in the range of 25-800 ºC under nitrogen atmosphere using a TA SDT 650 unit at a heating rate of 10 °C/min. In addition, to investigate the content of defects of the samples, TGA experiments were run from 50 to 1000 °C under oxygen atmosphere at a heating rate of 10 °C/min. The solid-state UV-Vis spectra of the metal phosphonates were recorded on HITACHI U-3900 spectrophotometer. Nitrogen adsorption desorption isotherms were analyzed using a Quantachrome NOVA 2200e at 77 K after degassing the samples at 100 °C for 8 h. Inductively coupled plasma-Optical emission spectrometer (ICP-OES) measurements were carried out on PE OPTMA8000DV. X-ray photoelectron spectroscopy (XPS) was performed on a VG ESCALABMK II spectrometer using an Al Kα (1486.6 eV) photon source. Scanning electron microscopy images were obtained on a FEI QUANTA FEG 400 and JEOL JSM-7500F. Transmission electron microscopy images were obtained on a FEI Tecnai G2 F20 at a voltage of 220 kV. Elemental mapping images were obtained on EDAX GENESIS.

Single-Crystal Structure Determination.

The diffraction intensity data set of compound **QAU-1-Ni-C** was collected on a Bruker SMART APEX II CCD diffractometer (Mo Kα radiation, λ= 0.71073 Å) at room temperature. The intensity data set of **QAU-1-Co-C** was collected on an XtaLAB Synergy Custom and a hybrid photon counting detector (HyPix-6000) at 100 K. The diffraction data were processed during data collection using CrysAlis Pro. SAINT was used for integration of intensity of reflections and scaling [2]. Absorption corrections were carried out with the program SADABS [3]. Crystal structures were solved by direct methods using SHELXS [4]. Subsequent difference Fourier analyses and least squares refinement with SHELXL-2013 [5] allowed for the location of the atom positions. All non-hydrogen atoms were refined with anisotropic thermal parameters. The hydrogen atoms on the water molecules were located from the difference Fourier map. All hydrogen atoms were refined using a riding model. The crystallographic details are summarized in Table S2. The data have been deposited in the Cambridge Crystallographic Data Centre (CCDC), deposition numbers CCDC 2081502-2081503 for compounds QAU-1-Ni-C and QAU-1-Co-C, respectively. These data can be obtained free of charge via www.ccdc.cam.ac.uk/data_request/cif, or by emailing data_request@ccdc.cam.ac.uk, or by contacting The Cambridge Crystallographic Data Centre, 12, Union Road, Cambridge CB2 1EZ, UK; fax: +44 1223336033.

Table S1. Raw materials in the syntheses of QAU-1-M.

Sample	Metal source	Ligand	Deionized water
QAU-1-Ni-C	$NiSO_4{\cdot}6H_2O$ (0.2 mmol)	H_6L (0.1mmol)	10 mL
QAU-1-Co-C	$CoCl_2.6H_2O$ (0.2 mmol)	H_6L (0.1mmol)	10 mL (100 μL HF)
QAU-1-Ni	$NiSO_4{\cdot}6H_2O$ (0.2 mmol)	H_6L (0.1 mmol)	30 mL
QAU-1-Co	$CoCl_2.6H_2O$ (0.2 mmol)	H_6L (0.1 mmol)	30 mL
QAU-1-Fe	$FeCl_2$ (0.2 mmol)	H_6L (0.1 mmol)	30 mL
QAU-1-NiCo(1:2)	$NiSO_4{\cdot}6H_2O$ (0.07 mmol) $CoCl_2.6H_2O$ (0.13 mmol)	H_6L (0.1 mmol)	30 mL
QAU-1-NiCo(1:1)	$NiSO_4{\cdot}6H_2O$ (0.1 mmol) $CoCl_2.6H_2O$ (0.1 mmol)	H_6L (0.1 mmol)	30 mL
QAU-1-NiCo(2:1)	$NiSO_4{\cdot}6H_2O$ (0.13 mmol) $CoCl_2.6H_2O$ (0.07 mmol)	H_6L (0.1 mmol)	30 mL
QAU-1-FeNi(1:4)	$NiSO_4{\cdot}6H_2O$ (0.16 mmol) $FeCl_2$ (0.04 mmol)	H_6L (0.1 mmol)	30 mL
QAU-1-FeNi(1:3)	$NiSO_4{\cdot}6H_2O$ (0.15 mmol) $FeCl_2$ (0.5 mmol)	H_6L (0.1 mmol)	30 mL
QAU-1-FeNi(1:2)	$NiSO_4{\cdot}6H_2O$ (0.13 mmol) $FeCl_2$ (0.07 mmol)	H_6L (0.1 mmol)	30 mL
QAU-1-FeNi(1:1)	$NiSO_4{\cdot}6H_2O$ (0.1 mmol) $FeCl_2$ (0.1 mmol)	H_6L (0.1 mmol)	30 mL
QAU-1-FeNi(2:1)	$NiSO_4{\cdot}6H_2O$ (0.07 mmol) $FeCl_2$ (0.13 mmol)	H_6L (0.1 mmol)	30 mL
QAU-1-FeCo(1:2)	$CoCl_2.6H_2O$ (0.13 mmol) $FeCl_2$ (0.07 mmol)	H_6L (0.1 mmol)	30 mL
QAU-1-FeCo(1:1)	$CoCl_2.6H_2O$ (0.1 mmol) $FeCl_2$ (0.1 mmol)	H_6L (0.1 mmol)	30 mL
QAU-1-FeCo(2:1)	$CoCl_2.6H_2O$ (0.07 mmol) $FeCl_2$ (0.13 mmol)	H_6L (0.1 mmol)	30 mL

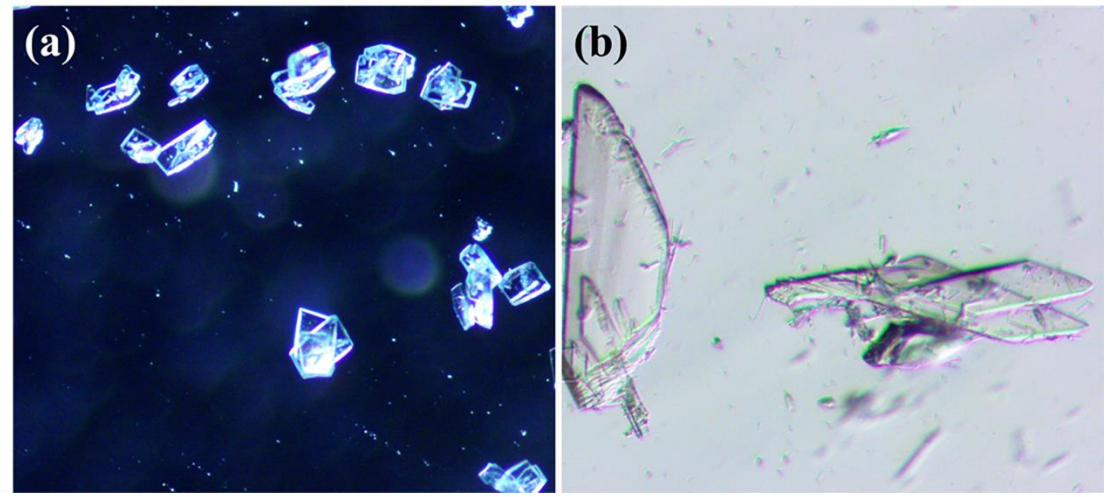

Figure S1. Microscope images of QAU-1-Ni-C (a) and QAU-1-Co-C (b).

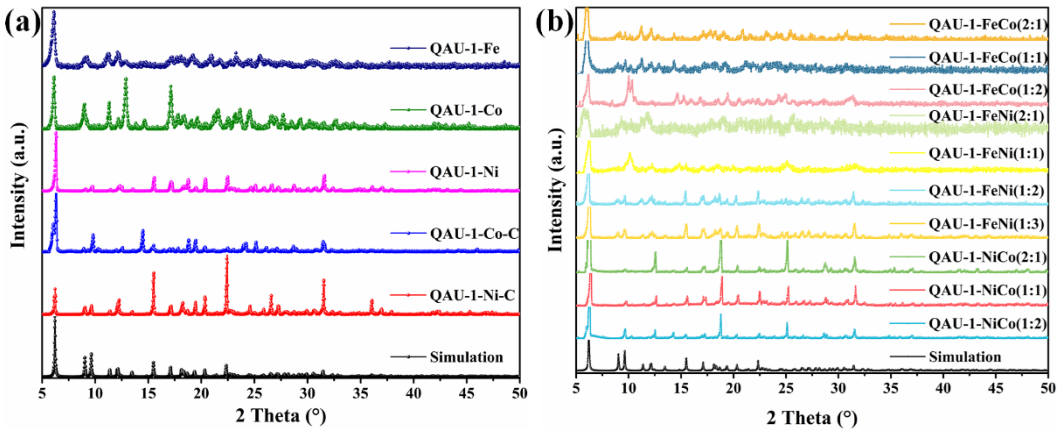

Figure S2. Power XRD patterns of as-prepared QAU-1-M samples.

Table S2. Crystal parameters of QAU-1-Ni-C and QAU-1-Co-C.

compound	**QAU-1-Ni-C**	**QAU-1-Co-C**
formula	$C_{24}H_{28}N_3NiO_{12}P_3$	$C_{24}H_{28}N_3CoO_{12}P_3$
fw	702.11	702.33
space group	*P*-1	*P*-1
a (Å)	10.2100(3)	10.1826(3)
b (Å)	10.2844(3)	10.4368(3)
c (Å)	15.2870(5)	15.2457(4)
α (deg)	73.7800(10)	74.176(3)
β (deg)	73.5220(10)	73.039(3)
γ (deg)	79.6770(10)	79.044(2)
V (Å^3)	1469.26(8)	1480.23(8)
Z	2	2
D_{calcd}/g cm^{-3}	1.587	1.576
abs coeff /mm^{-1}	0.891	0.808
F(000)	724	722
theta range	3.102-24.996	1.435-24.993
completeness /%	96.5	92.5
reflns collected	26732	16659
independent reflns/Rint	5138/0.0431	4959/0.0749
GOF on F^2	1.029	0.998
final *R* indices [$I>2\sigma(I)$]: R_1, wR_2	0.0401, 0.0997	0.0545, 0.1344
R indices (all data): R_1, wR_2	0.0565, 0.1076	0.0747, 0.1433

$^a R_1 = \Sigma||F_o|-|F_c||/\Sigma|F_o|$. $^b \omega R_2=\{\Sigma[\omega(F_o^2-F_c^2)^2]/\Sigma\omega(F_o^2)^2\}^{1/2}$

Structural description of crystal QAU-1-Ni-C and QAU-1-Co-C.

The crystal structure of **QAU-1-Ni-C (**denoted as IEF-13**)** has been reported in a very recent paper [6]. Here the crystal structure of QAU-1-Co-C is described in detail. QAU-1-Co-C crystallizes in triclinic space group *P*-1 with two molecules in each lattice. In the asymmetric unit, there are a crystallographic independent cobalt(II) ion, one double deprotonated trisphosphonate ligand (H_4L), two aqua ligands and one lattice water molecule, indicating a formula of $[Co(H_4L)(H_2O)_2]\cdot H_2O$. The cobalt(II) ion is octahedrally coordinated by four phosphonate oxygen atoms from

trisphosphonate ligands and two aqua ligands. The Co-O bond lengths and O-Co-O bond angles are in the ranges of 2.029(3)-2.145(3) Å and 79.47(9)-176.21(12)^{o} (Table S3) respectively, which are all comparable to those reported in the literatures[7]. The trisphosphonate ligand is double deprotonated. Two of the three phosphonate groups in the ligand are monodentate whereas the third one is bidentate. Its coordination mode can be denoted as: μ^4:η^0:η^1:η^0:η^0:η^1:η^0:η^0:η^2:η^0, which means the phosphonate ligand bridges four cobalt ions with its three phosphonate oxygen atoms (see Figure S3). Neighboring two nickel ions form a dimer with a Co···Co bond length of 3.271 Å through the linkage of six trisphosphonate ligands. These dimers are linked by the ligands to form a two-dimensional layer in *bc*-plane (see Figure S4a) which are further assembled into a three-dimensional supramolecular crystal structure (see Figure S4b) via plenty of π···π interactions, traditional and untraditional hydrogen bonds (see Table S4-S6). From the topology view, the dimers and the trisphosponate ligands can be viewed as 6-connected and 3-connected nodes, respectively. Therefore, the two-dimensional layer is binodal net with a short vertex symbol of (4^6, 4^3) (see Figure 4d).

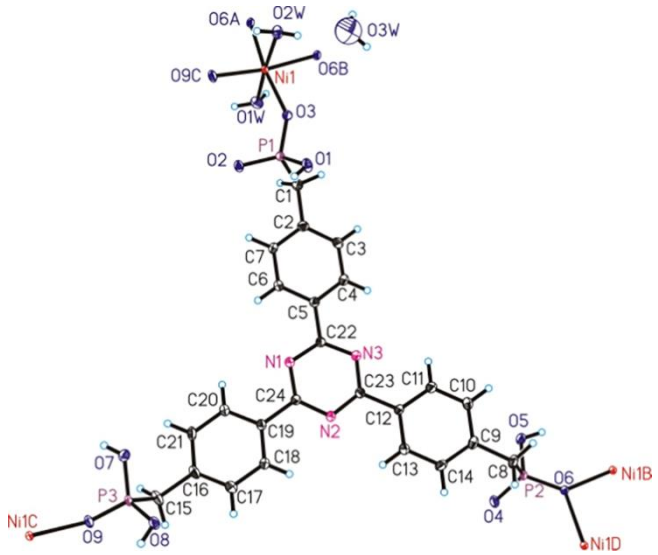

Figure S3. Coordination modes of the trisphosphonate ligand and the Co center. Symmetry transformations used to generate equivalent atoms: A: 1+x, -1+y, 1+z; B: -x, 2-y, -1-z; C: -x, 3-y, -z; D: -1+x, 1+y, -1+z

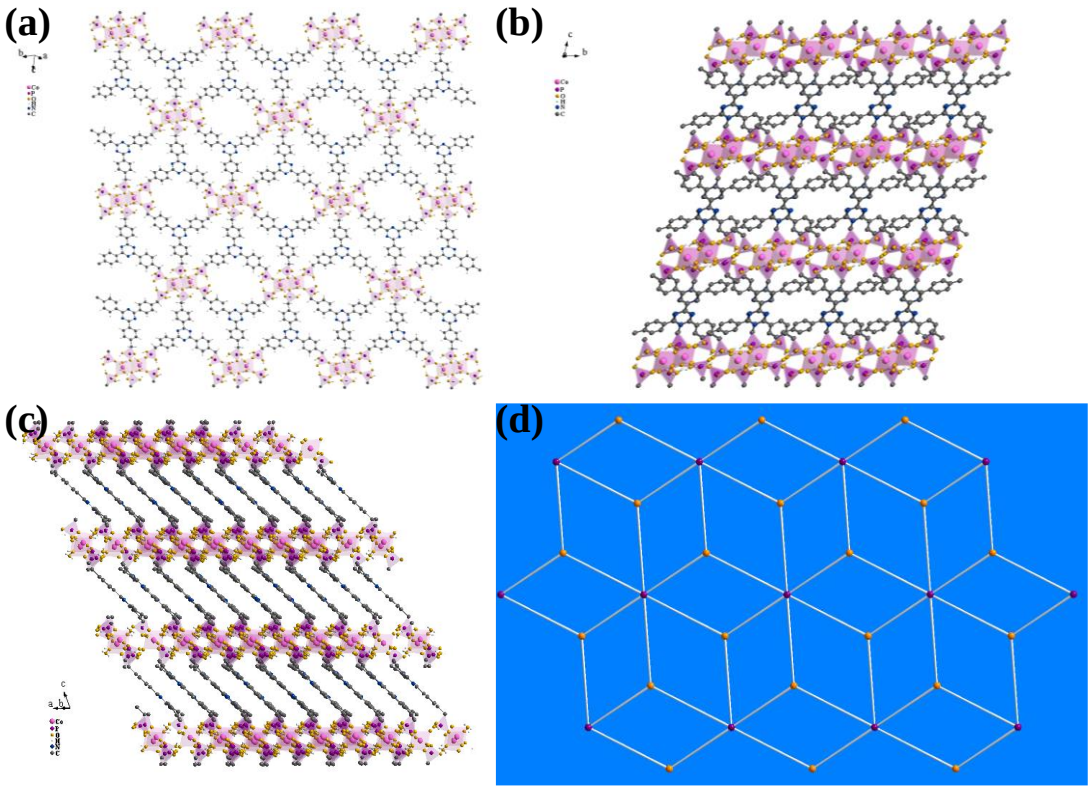

Figure S4. Two-dimensional layer (a), three-dimensional supramolecular crystal structure viewing along *a*-direction (b) and *b*-direction (c), and schematic representation of the topology (d) of QAU-1-Co-C.

Table S3. Selected bonds (Å) and angels (°) of QAU-1-Ni-C and QAU-1-Co-C.

QAU-1-Ni-C			
Ni(1)-O(9)#1	2.004(2)	Ni(1)-O(6)#2	2.087(2)
Ni(1)-O(3)	2.042(2)	Ni(1)-O(2W)	2.091(2)
Ni(1)-O(1W)	2.080(2)	Ni(1)-O(6)#3	2.093(2)
O(9)#1-Ni(1)-O(3)	93.73(9)	O(1W)-Ni(1)-O(2W)	175.21(9)
O(9)#1-Ni(1)-O(1W)	96.65(10)	O(6)#2-Ni(1)-O(2W)	88.63(9)
O(3)-Ni(1)-O(1W)	89.88(10)	O(9)#1-Ni(1)-O(6)#3	172.37(9)
O(9)#1-Ni(1)-O(6)#2	94.69(8)	O(3)-Ni(1)-O(6)#3	91.81(8)
O(3)-Ni(1)-O(6)#2	171.56(8)	O(1W)-Ni(1)-O(6)#3	88.60(9)
O(1W)-Ni(1)-O(6)#2	89.70(9)	O(6)#2-Ni(1)-O(6)#3	79.75(8)
O(9)#1-Ni(1)-O(2W)	87.96(9)	O(2W)-Ni(1)-O(6)#3	86.69(9)
O(3)-Ni(1)-O(2W)	91.11(10)		
QAU-1-Co-C			
Co(1)-O(6)#1	2.029(3)	O(3)#2-Co(1)-O(3W)	89.72(11)
Co(1)-O(9)	2.046(3)	O(6)#1-Co(1)-O(2W)	95.69(12)
Co(1)-O(3)#2	2.108(3)	O(9)-Co(1)-O(2W)	88.77(12)
Co(1)-O(3W)	2.133(3)	O(3)#2-Co(1)-O(2W)	88.82(11)
Co(1)-O(2W)	2.136(3)	O(3W)-Co(1)-O(2W)	176.21(12)
Co(1)-O(3)#3	2.145(3)	O(6)#1-Co(1)-O(3)#3	171.40(10)
O(6)#1-Co(1)-O(9)	95.45(11)	O(9)-Co(1)-O(3)#3	90.50(10)
O(6)#1-Co(1)-O(3)#2	94.80(10)	O(3)#2-Co(1)-O(3)#3	79.47(9)
O(9)-Co(1)-O(3)#2	169.66(10)	O(3W)-Co(1)-O(3)#3	85.66(11)

O(6)#1-Co(1)-O(3W)	87.92(11)	O(2W)-Co(1)-O(3)#3	90.63(12)
O(9)-Co(1)-O(3W)	92.05(12)		

Symmetry transformations used to generate equivalent atoms: #1 -x+3, -y, -z+2; #2 x+1, y-1, z+1; #3 -x+3, -y-1, -z+1; #4 x-1, y+1, z-1.

Table S4. π···π interactions in QAU-1-Ni-C and QAU-1-Co-C.

Cg(I)···Cg(J)	Cg···Cg	Alpha	Beta	Gamma	CgI_Perp	CgJ_Perp
QAU-1-Ni-C						
Cg1···Cg1#1	3.7630(17)	0.03(15)	29.1	29.1	-3.2873(12)	-3.2873(12)
Cg1···Cg2#1	4.8706(17)	7.28(16)	46.8	52.9	2.9358(13)	-3.3335(14)
Cg1···Cg3#2	5.118(2)	4.14(17)	46.0	47.1	3.4824(12)	3.5563(15)
Cg1···Cg3#1	5.093(2)	4.14(17)	47.5	48.7	-3.3612(12)	-3.4408(15)
Cg2···Cg1#1	4.8707(17)	7.28(16)	52.9	46.8	-3.3335(14)	2.9358(13)
Cg2···Cg3#1	4.147(2)	10.55(18)	29.3	36.9	-3.3181(14)	3.6164(16)
Cg2···Cg4#3	5.239(2)	18.44(17)	44.3	60.9	-2.5472(14)	-3.7466(16)
Cg3···Cg1#2	5.118(2)	4.14(17)	47.1	46.0	3.5563(15)	3.4824(12)
Cg3···Cg1#1	5.093(2)	4.14(17)	48.7	47.5	-3.4407(15)	-3.3612(12)
Cg3···Cg2#1	4.147(2)	10.55(18)	36.9	29.3	3.6164(16)	-3.3181(14)
Cg3···Cg3#2	3.897(2)	0.03(18)	25.1	25.1	3.5274(15)	3.5274(15)
QAU-1-Co-C						
Cg(1)···Cg(4)#1	5.6201	17	14.4	20.1	-5.2792	-5.4429
Cg(1)···Cg(4)#2	5.6201	17	14.4	20.1	-5.2792	5.4429
Cg(2)···Cg(2)#3	3.7113	0	27.9	27.9	3.2803	3.2803
Cg(2)··· Cg(3) #3	5.0358	4	46.8	48.7	3.3268	3.4500
Cg(2)···Cg(3) #2	5.1476	4	46.3	48.0	-3.4416	-3.5589
Cg(2)··· Cg(5) #3	4.9200	8	47.9	53.9	-2.8981	3.3007
Cg(3)···Cg(2) #3	5.0358	4	48.7	46.8	3.4500	3.3269
Cg(3)··· Cg(2) #2	5.1476	4	48.0	46.3	-3.5589	-3.4416
Cg(3)··· Cg(3) #2	3.8662	0	25.3	25.3	-3.4952	-3.4952
Cg(3)···Cg(5) #3	4.1929	12	37.7	29.8	-3.6388	3.3160
Cg(4)··· Cg(1) #4	5.6201	17	20.1	14.4	-5.4429	-5.2792
Cg(4)··· Cg(1) #2	5.6201	17	20.1	14.4	5.4429	-5.2792
Cg(5)···Cg(2) #3	4.9200	8	53.9	47.9	3.3007	-2.8981
Cg(5)···Cg(3) #3	4.1929	12	29.8	37.7	3.3160	-3.6388
Cg(5)··· Cg(4) #5	5.3378	20	44.1	62.1	2.4953	3.8357

Cg(I) = Plane number I (= ring number in () above)
Alpha = Dihedral Angle between Planes I and J (Deg)
Beta = Angle Cg(I)-->Cg(J) or Cg(I)-->Me vector and normal to plane I (Deg)
Gamma = Angle Cg(I)-->Cg(J) vector and normal to plane J (Deg)
Cg···Cg = Distance between ring Centroids (Ang.)
CgI_Perp = Perpendicular distance of Cg(I) on ring J (Ang.)
CgJ_Perp = Perpendicular distance of Cg(J) on ring I (Ang.)
For QAU-1-Ni-C:
Cg1: N1-C22-N3-C23-N2-C24→
Cg2: C2-C3-C4-C5-C6-C7→
Cg3: C9-C10-C11-C12-C13-C14→
Cg4: C16-C17-C18-C19-C20-C21→
#1 = 3-x,-y,1-z; #2= 2-x,-y,1-z; #3= x,-1+y,z.
For QAU-1-Co-C:
Cg1: Co(1)-O(3)-Co(1)-O(3)→
Cg2: N(1)-C(1)-N(2)-C(17)-N(3)-C(9)→
Cg3: C(2)-C(3)-C(4)-C(5)-C(6)-C(7)→
Cg4: C(10)-C(11)-C(12)-C(13)-C(14)-C(15)→
Cg5: C(18)-C(19)-C(20)-C(21)-C(22)-C(23)→
#1 = X, Y, 1+Z; #2 = 1-X, 1-Y, 1-Z; #3 = -X, 1-Y, 1-Z; #4 = X, Y, -1+Z; #5 = X, 1+Y, Z.

Table S5. Hydrogen bonds in QAU-1-Ni-C and QAU-1-Co-C.

Donor- H···Acceptor	D-H	H···A	D···A	D-H···A
QAU-1-Ni-C				
O1-H1C···O2#1	0.82	1.77	2.573(3)	166
O1W-H1W···O2W#2	0.85	2.30	3.057(3)	148
O1W-H2W···O7#3	0.85	2.21	2.980(3)	150
O2W-H3W···O3W	0.85	1.85	2.673(7)	162
O2W-H4W···O9#4	0.85	2.55	2.846(3)	101
O2W-H4W···N1#1	0.85	2.45	3.182(4)	144
O5-H5A···O3#5	0.82	1.72	2.535(3)	176
O3W-H6W···O3W#6	0.85	2.57	3.116(9)	123
O7-H7B···O2#4	0.82	1.74	2.555(3)	178
O8-H8C···O4#7	0.82	1.65	2.466(3)	179
C1-H1A···O8#3	0.97	2.49	3.339(4)	146
C6-H6A···N1	0.93	2.46	2.785(5)	101
C7-H7A···O4#8	0.93	2.57	3.329(5)	139
C11-H11A···N3	0.93	2.53	2.842(5)	100
C13-H13A···N2	0.93	2.45	2.774(5)	101
C20-H20A···N1	0.93	2.47	2.792(4)	100
QAU-1-Co-C				
O(1)-H(1A)···O(9)#1	0.82	1.72	2.5428	176
O(2W)-H(3W)···O(4)#2	0.85	2.15	2.9934	169
O(4)-H(4B)···O(7)#3	0.82	1.74	2.5574	176
O(2W)-H(4W)···O(3W)#4	0.85	2.39	3.1464	149
O(5)-H(5A)···O(2)#5	0.82	1.65	2.4715	177
O(3W)-H(5W)···O(2W)#4	0.85	2.59	3.1464	124
O(3W)-H(6W)···O(9)#6	0.85	2.55	3.0081	114
O(8)-H(8C)···O(7)#7	0.82	1.77	2.5738	167
C(3)-H(3A)···N(2)	0.93	2.53	2.8434	100
C(7)-H(7A)···N(1)	0.93	2.45	2.7797	101
C(15)-H(15A)···N(3)	0.93	2.48	2.7994	101
C(22)-H(22A)···O(2)#8	0.93	2.60	3.3325	136
C(23)-H(23A)···N(3)	0.93	2.48	2.7983	100
C(24)-H(24A)···O(5)#9	0.97	2.50	3.3525	146

Translation of ARU-Code to CIF and Equivalent Position Code

For QAU-1-Ni-C:

#1 = 3-x, -1-y, 2-z; #2 = 4-x, -2-y, 2-z; #3 = 1+x,-1+y,z; #4 = 3-x,-y,2-z; #5 = 3-x, -1-y, 1-z; #6 = 3-x, -2-y, 2-z; #7 = 2-x, 1-y, 1-z; #8 = 3-x, -y, 1-z.

For QAU-1-Co-C:

#1 = -x, 2-y, 1-z; #2 = x, y, 1+z; #3 = -x, 1-y, -z; #4 = 1-x, 1-y, 2-z; #5 = 1-x, -y, 1-z; #6 = 1+x, -1+y, 1+z; #7 = -x, 2-y, -z; #8 = -x, 1-y, 1-z; #9 = -1+x, 1+y, z.

Table S6. C-H···π Interactions in QAU-1-Ni-C and QAU-1-Co-C.

X-H···Cg(J)	H···Cg	H-Perp	Gamma	X-H···Cg	X···Cg	X-H···Pi
QAU-1-Ni-C						
C15-H15B···Cg2#1	2.82	-2.51	27.11	165	3.761(5)	49
QAU-1-Co-C						
O(2W)-H(4W)···Cg(1)	2.60	-2.46	19.08	86	2.6821	22

O(2W)-H(4W)···Cg(1)#1	2.60	2.46	19.08	86	2.6821	22
O(3W)-H(5W)···Cg(1)	2.49	2.27	24.29	89	2.6186	10
O(3W)-H(5W)···Cg(1)#1	2.49	-2.27	24.29	89	2.6186	10
C(16)-H(16B)···Cg(5)#2	2.83	2.51	27.71	167	3.7826	50

Cg(J) = Center of gravity of ring J (Plane number above)
H-Perp = Perpendicular distance of H to ring plane J
Gamma = Angle between Cg-H vector and ring J normal
X-H···Cg = X-H-Cg angle (degrees)
X···Cg = Distance of X to Cg (Angstrom)
X-H, Pi = Angle of the X-H bond with the Pi-plane
For QAU-1-Ni-C :#1= x,1+y, z.
For QAU-1-Co-C : #1 = 1-X, 1-Y, 2-Z; #2 = X, -1+Y, Z

Table S7 Elemental analysis results of the defective samples QAU-1-M by ICP-OES

Samples	Ni (wt%)	Co (wt%)	Fe (wt%)	M:M’	
QAU-1-Ni	8.9	--	--	--	
QAU-1-Co	--	1.4	--	--	
QAU-1-Fe	--	--	13.0	--	
QAU-1-NiCo(1:2)	2.9	7.3	--	Ni:Co	0.39
QAU-1-NiCo(1:1)	4.4	5.3	--	Ni:Co	0.83
QAU-1-NiCo(2:1)	6.5	3.4	--	Ni:Co	1.95
QAU-1-FeNi(1:3)	7.3	--	2.8	Fe:Ni	0.40
QAU-1-FeNi(1:2)	2.4	--	4.0	Fe:Ni	1.77
QAU-1-FeNi(1:1)	2.4	--	7.0	Fe:Ni	3.07
QAU-1-FeNi(2:1)	1.5	--	11.5	Fe:Ni	7.91
QAU-1-FeCo(1:2)	--	6.3	4.6	Fe:Co	0.76
QAU-1-FeCo(1:1)	--	3.7	6.2	Fe:Co	1.77
QAU-1-FeCo(2:1)	--	0.4	10.8	Fe:Co	26.73

Table S8 Summary of the electrocatalytic performance of various QAU-1-M catalysts.

Catalyst	η_{10} (mV)	Tafel slope (mV dec^{-1})	Rs (ohm)	Rct (ohm)	C_{dl} (mF cm^{-2})	TOF (s^{-1})
QAU-1-Ni	315	105	1.4	6.43	3.91	0.0071
QAU-1-Co	346	63	1.0	7.93	8.03	0.0016
QAU-1-Fe	304	52	1.1	1.01	4.49	0.0077
QAU-1-NiCo(1:2)	335	82	1.1	6.07	12.75	0.0036
QAU-1-NiCo(1:1)	332	78	1.1	6.08	7.02	0.0034
QAU-1-NiCo(2:1)	332	74	1.3	5.54	4.91	0.0034
QAU-1-FeNi(1:3)	261	65	1.3	0.62	4.7	0.0311

QAU-1-FeNi(1:2)	230	47	1.2	0.58	8.48	0.0356
QAU-1-FeNi(1:1)	274	67	1.2	1.03	4.34	0.0220
QAU-1-FeNi(2:1)	299	52	1.1	0.70	4.2	0.0093
QAU-1-FeCo(1:2)	278	51	1.4	0.71	4.35	0.0252
QAU-1-FeCo(1:1)	274	51	1.4	0.76	4.36	0.0283
QAU-1-FeCo(2:1)	291	60	1.4	0.93	3.66	0.0128

Table S9 Comparison of the C_{dl} values determined from EIS (C_{dl}-EIS) and those from CV curves (C_{dl}-CV).

Catalyst	**QAU-1-FeNi(1:2)**	**QAU-1-FeNi(1:1)**	**QAU-1-FeNi(2:1)**	**QAU-1-FeNi(1:3)**	**QAU-1-FeCo(1:2)**	**QAU-1-FeCo(1:1)**	**QAU-1-FeCo(2:1)**
C_{dl}-CV (mF cm^{-2})	8.48	4.34	4.2	4.7	4.35	4.36	3.66
C_{dl}-EIS (mF cm^{-2})	8.83	5.08	4.70	7.22	7.37	6.96	5.90
Catalyst	**QAU-1-Ni**	**QAU-1-Co**	**QAU-1-Fe**	**QAU-1-NiCo(1:2)**	**QAU-1-NiCo(1:1)**	**QAU-1-NiCo(2:1)**	
C_{dl}-CV (mF cm^{-2})	3.91	8.03	4.49	12.75	7.02	4.91	
C_{dl}-EIS (mF cm^{-2})	7.35	7.49	4.74	7.54	7.53	8.12	

C_{dl}-EIS values are calculated from the follow formula:

$$C_{dl} = \frac{1}{2\pi f Z''}$$

Where f is alternating current frequency, Z'' is the impedance of the imaginary part.

Table S10 Comparison of the OER activity of phosphonates materials.

Catalysts	Electrolyte	Working electrode	Overpotential (mV)	Tafel slope (mV $dec^{-1)}$	Ref.
NiFe16-phenylphosphonate	1.0 M KOH	GEC	240	40	[8]
CoPIm	1.0 M KOH	Carbon Paper	334	58.6	[9]
CoNTO-1-4	1.0 M KOH	Carbon Paper	312	62.1	[10]
NiPPA	1.0 M KOH	Carbon Paper	434	116.7	[11]
CoPi-1	1.0 M KOH	GCE	380	58.7	[12]
CoNiPP-600	1.0 M KOH	GCE	264	60	[13]
H_3LCoCN800	1.0 M KOH	Ni Foam	260	64	[14]
$Co_3(O_3PCH_2$-NC_4H_7-	0.1 PBS	GCE	484#	83	[15]

$CO_2)_2 \cdot 4H_2O$					
$Co[(CH_3PO_3)(H_2O)]$	Water-saturated [BMIM][PF_6]	GCE	~1.45*	--	[16]
$Co[(C_2H_5PO_3)(H_2O)]$	Water-saturated [BMIM][PF_6]	GCE	~1.45*	--	[16]
$Co[(C_4H_9PO_3)(H_2O)]$	Water-saturated [BMIM][PF_6]	GCE	~1.50*	--	[16]
$Co[(C_6H_5PO_3)(H_2O)]$	Water-saturated [BMIM][PF_6]	GCE	~1.55*	--	[16]
$Co_3(OH)_2(HPO_4)_2$	1.0 M KOH	GCE	290	82	[17]
QAU-1-Ni	1.0 M KOH	Ni Foam	315	105	This work
QAU-1-Co	1.0 M KOH	Ni Foam	346	63	
QAU-1-Fe	1.0 M KOH	Ni Foam	304	52	
QAU-1-NiCo(2:1)	1.0 M KOH	Ni Foam	332	74	
QAU-1-FeNi(1:2)	1.0 M KOH	Ni Foam	230	47	
QAU-1-FeCo(1:1)	1.0 M KOH	Ni Foam	274	51	

: overpotential at a current density of 1 mA cm^{-2}; * : E vs Fe/Fe^+ (V) at a current of 50 μA.

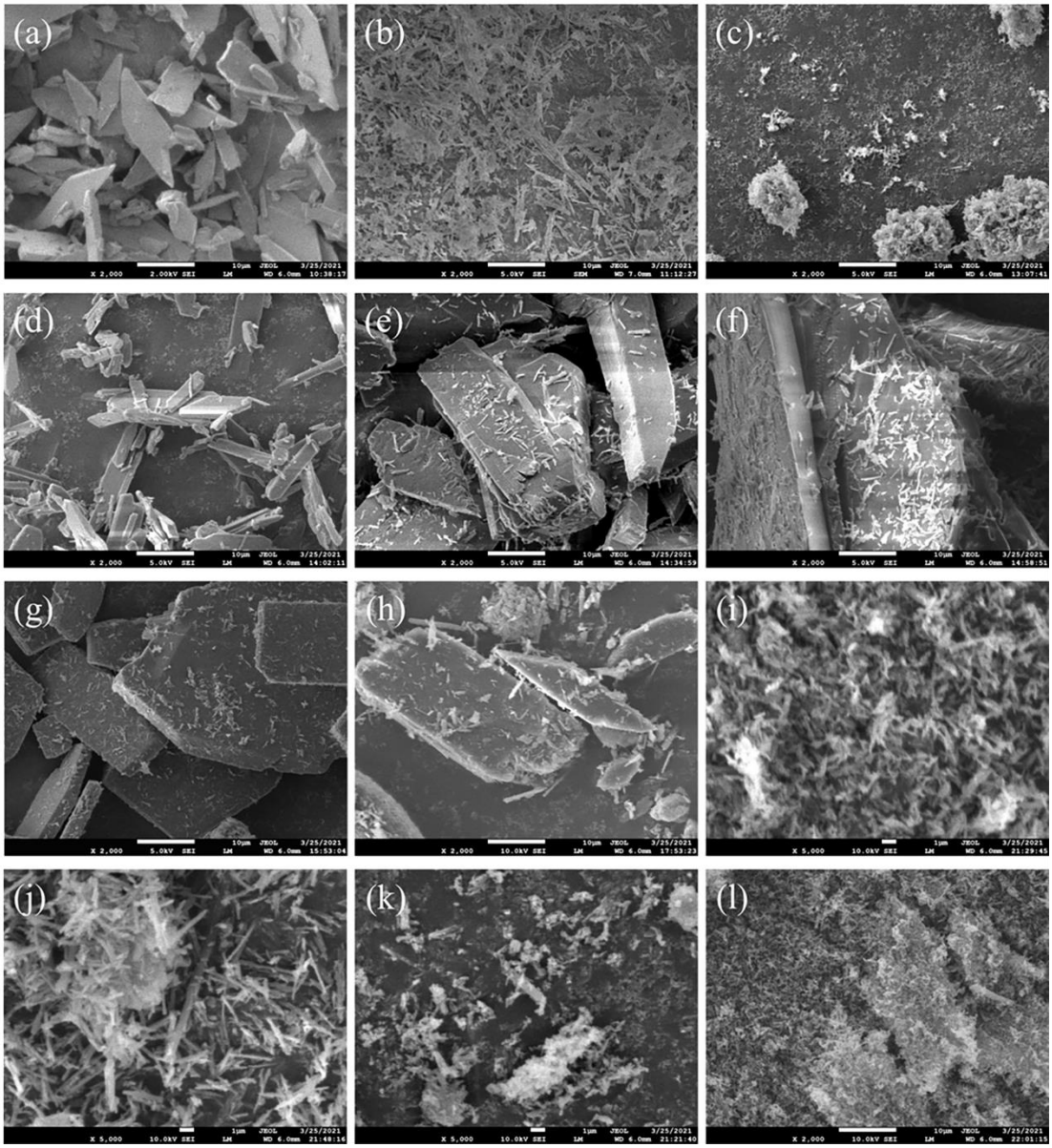

Figure S5. SEM images of (a) QAU-1-Ni, (b) QAU-1-Co, (c) QAU-1-Fe, (d)

QAU-1-NiCo(1:2), (e) QAU-1-NiCo(1:1), (f) QAU-1-NiCo(2:1), (g) QAU-1-FeNi(1:3), (h) QAU-1-FeNi(1:1), (i) QAU-1-FeNi(2:1), (j) QAU-1-NiCo(1:2), (k) QAU-1-NiCo(1:1), (l) QAU-1-NiCo(2:1).

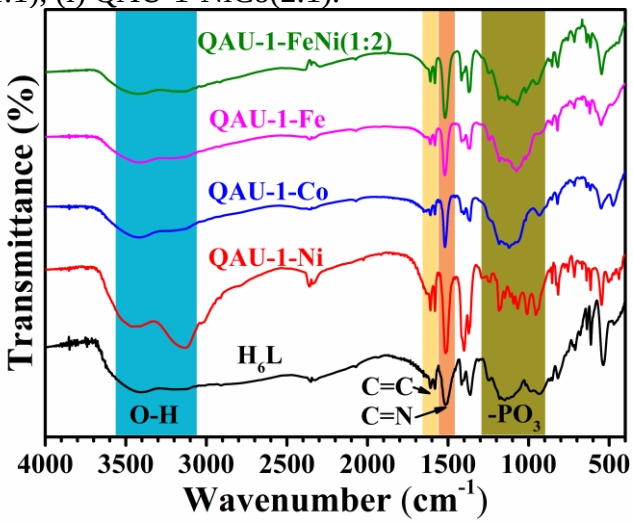

Figure S6. FT-IR spectra of QAU-1-Ni, QAU-1-Co, QAU-1-Fe, QAU-1-FeNi(1:2) and ligand H_6L.

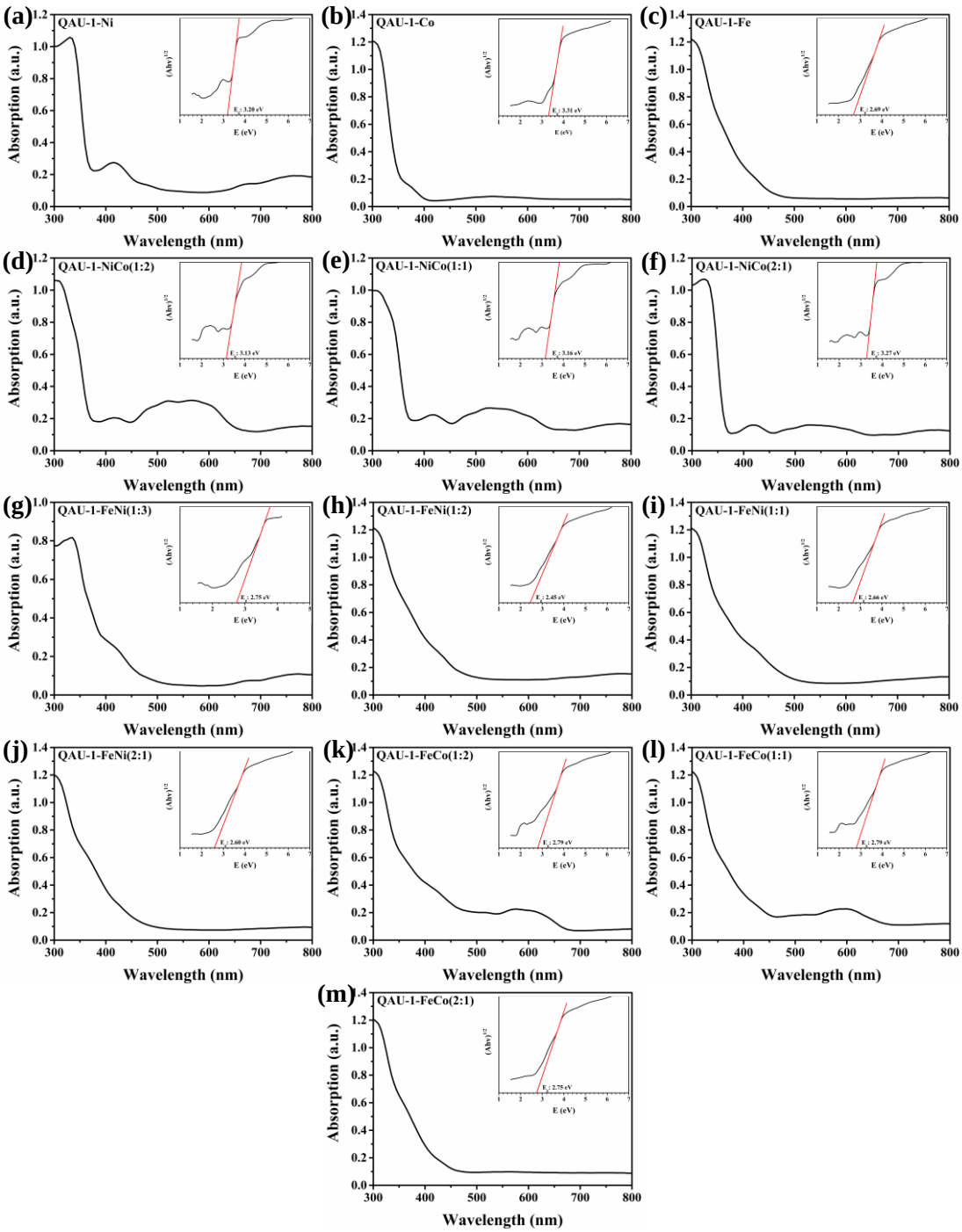

Figure S7. UV-vis absorption spectra and the corresponding E_g values of as-prepared QAU-1-M samples.

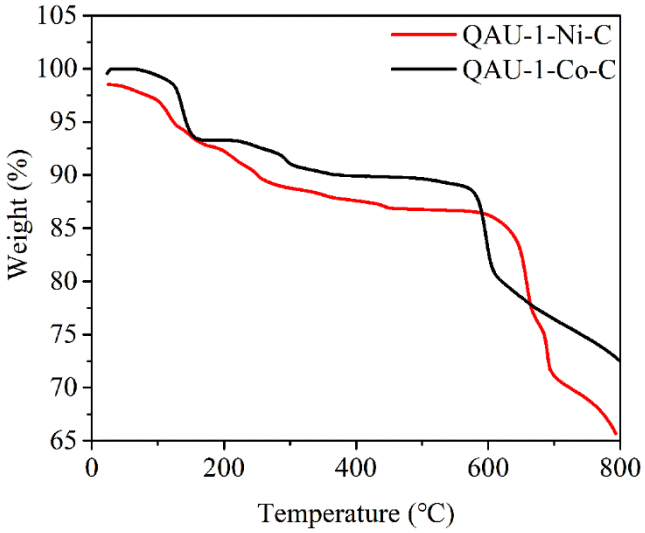

Figure S8. TGA curve of QAU-Ni-C and QAU-Co-C under nitrogen atmosphere.

Defect content determination of the samples:

The weight loss percentage that the samples will lose during the second stage can be calculated by following equations:

$$Ideal\ weight\ loss = \frac{M_{(C_{24}H_{28}N_3O_{12}P_3M)} - M_{(3H_2O)} - M_{(M(PO_3)_x)}}{M_{(C_{24}H_{28}N_3O_{12}P_3M)}} * 100\%$$

$$M_{(M(PO_3)_x)} = \frac{M_{(Ni(PO_3)_2)} * Wt_{(Ni)}\% + M_{(Co(PO_3)_2)} * Wt_{(Co)}\% + M_{(Fe(PO_3)_3)} * Wt_{(Fe)}\%}{Wt_{(Ni)}\% + Wt_{(Co)}\% + Wt_{(Fe)}\%}$$

Where $Wt_{(M)}\%$ is the value obtained by the ICP-OES.

$$Number\ of\ defects\ per\ formula\ unit = \frac{Ideal\ weight\ loss - Actual\ weight\ loss}{Ideal\ weight\ loss}$$

$$Number\ of\ ligands\ per\ formula\ unit = 1 - Number\ of\ defects\ per\ formula\ unit$$

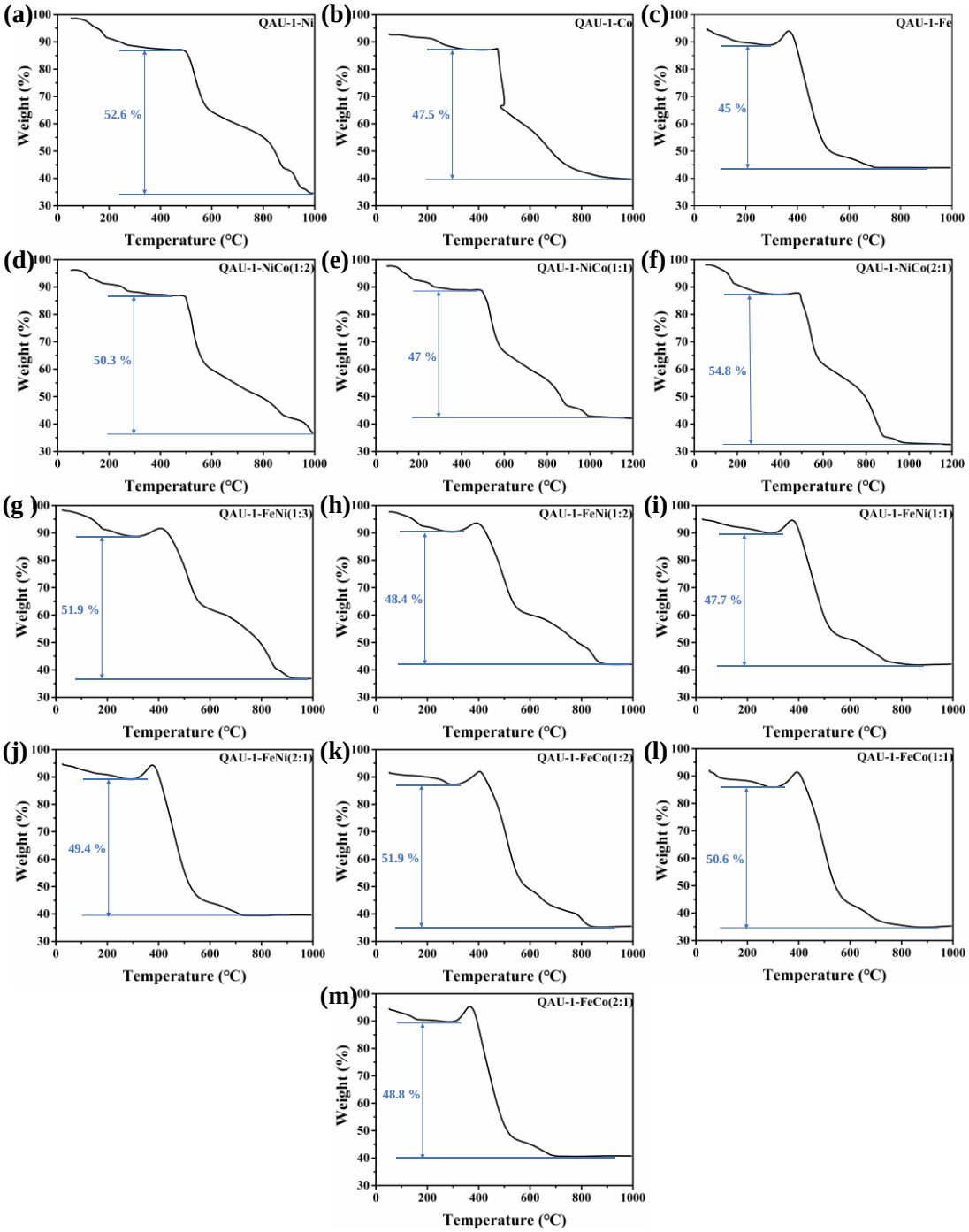

Figure S9. TGA curves of as-prepared QAU-1-M samples under oxygen atmosphere.

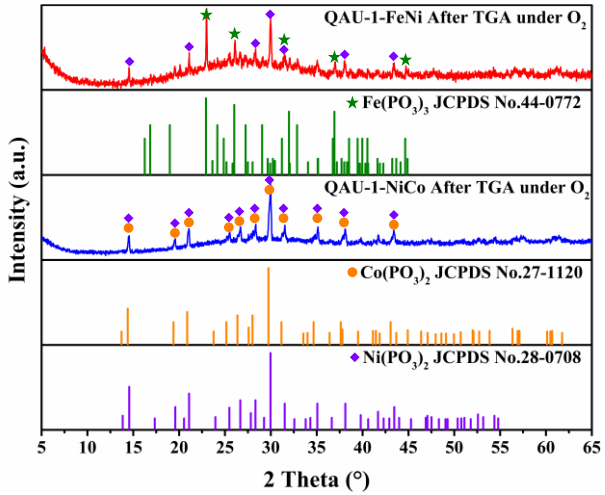

Figure S10. The XRD patterns of QAU-1-NiCo and QAU-1-FeNi after TGA under oxygen atmosphere and standard cards.

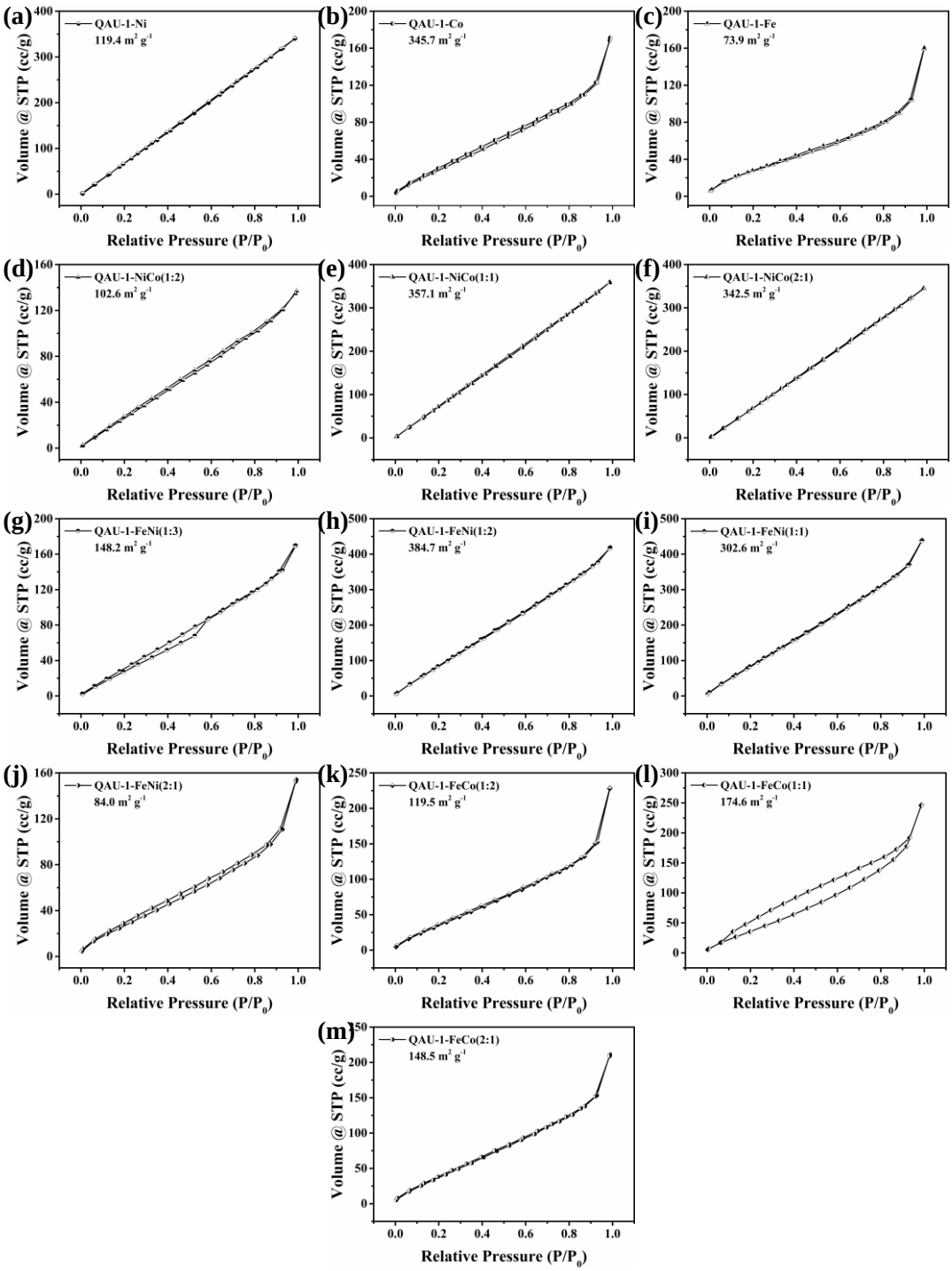

Figure S11. N_2 adsorption-desorption isotherms of as-prepared QAU-1-M samples.

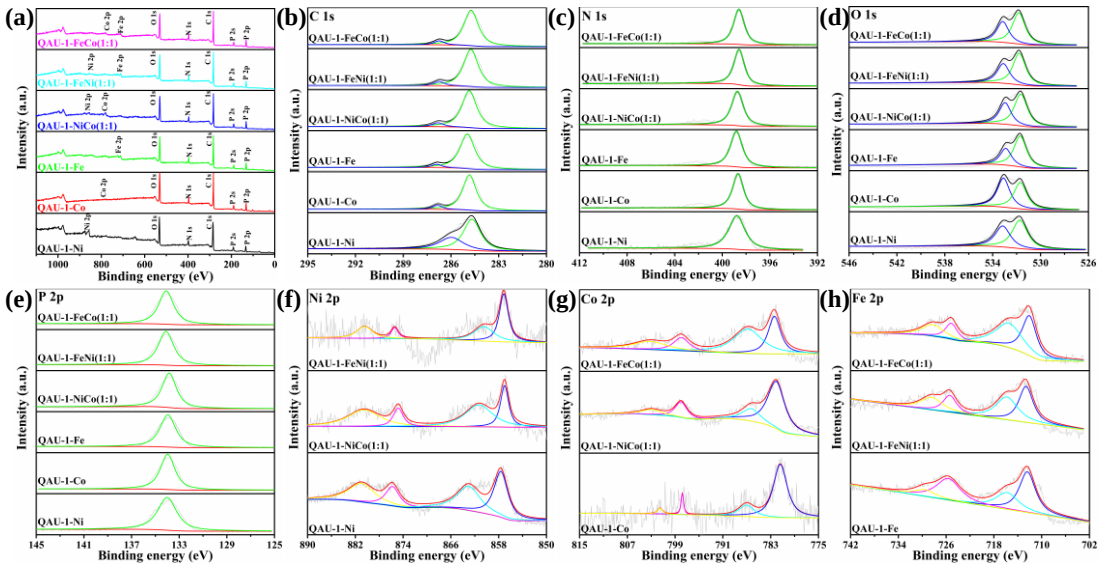

Figure S12. XPS survey spectra of QAU-1-Ni, QAU-1-Co, QAU-1-Fe, QAU-1-NiCo(1:1), QAU-1-FeCo(1:1) and QAU-1-FeNi(1:1).

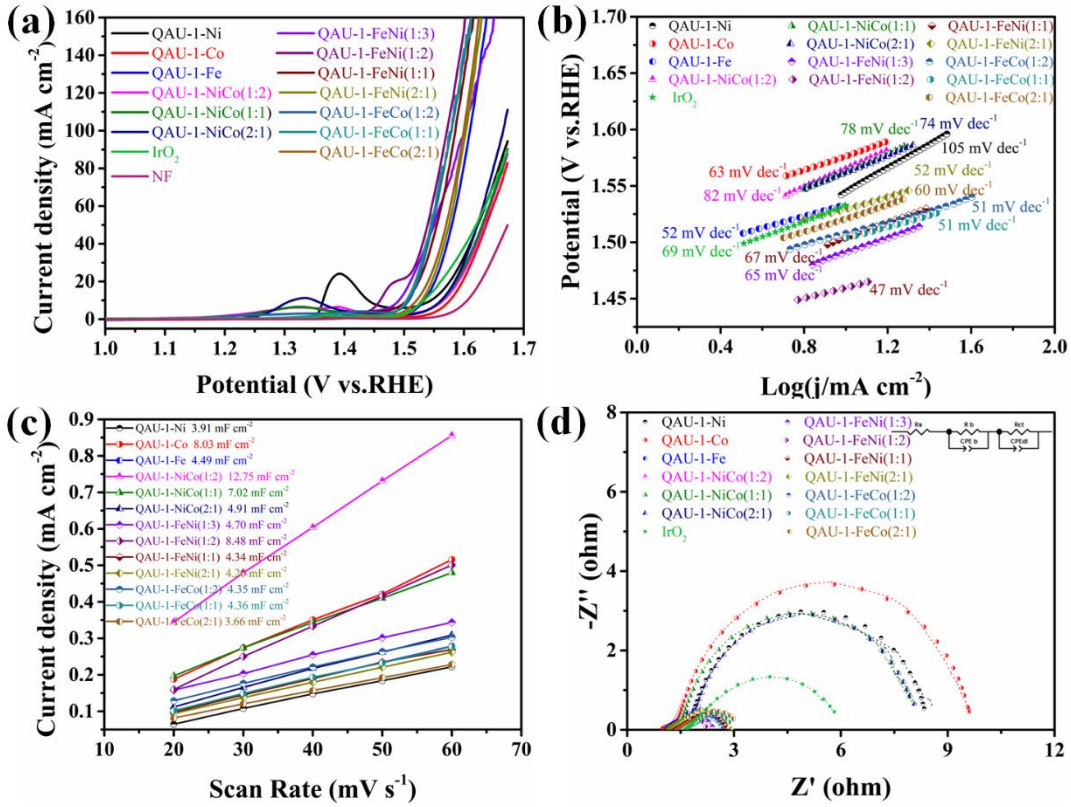

Figure S13. (a) LSV polarization curves of as-prepared QAU-1-M catalysts, commercial IrO_2 and NF; (b) the corresponding Tafel slope; (c) plots of the capacitive currents as a function of scan rate of as-prepared QAU-1-M catalysts; (d) EIS Nyquist plots of as-prepared QAU-1-M catalysts and IrO_2, scatter points are the fitted curves and dotted lines are experimentally obtained data.

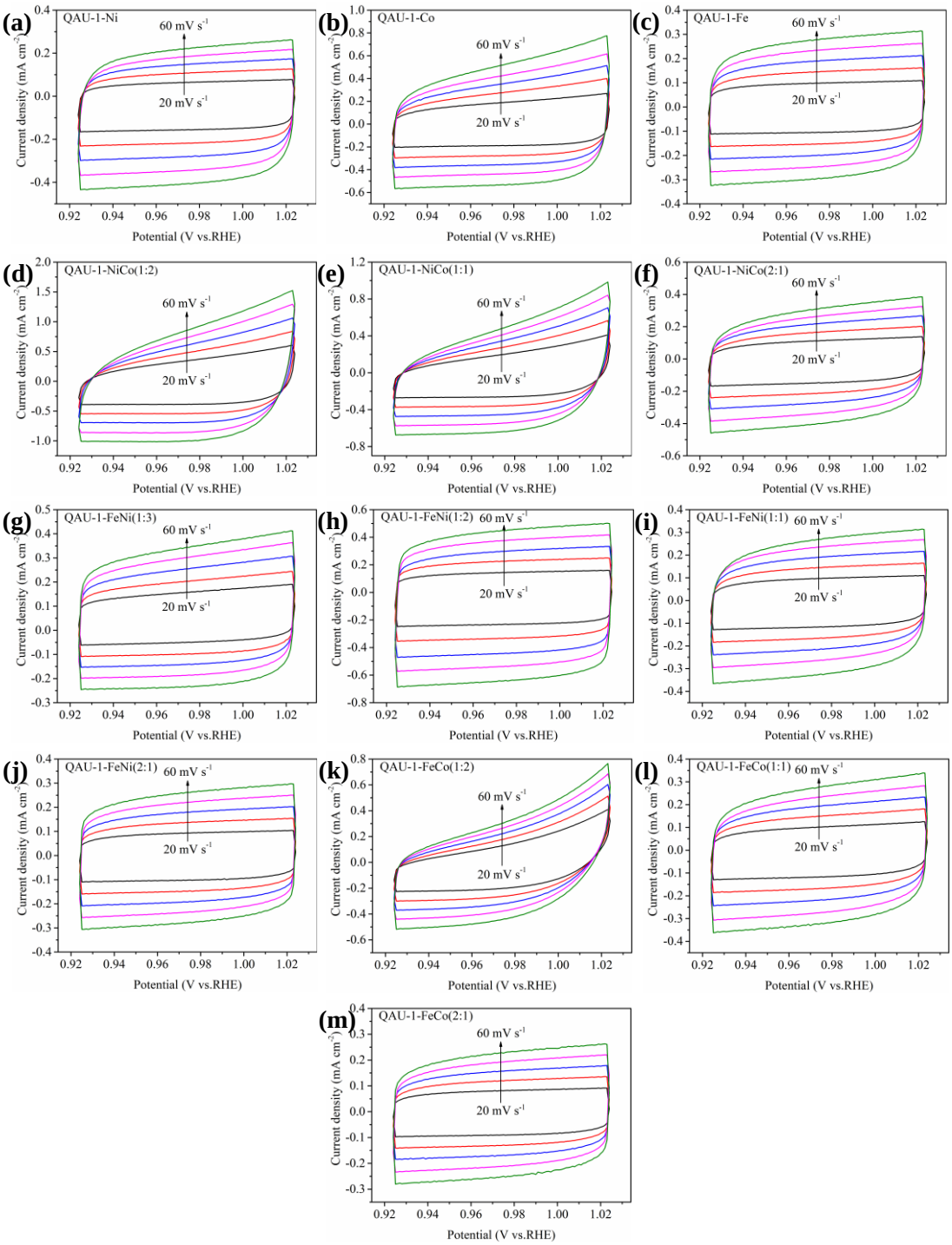

Figure S14. Cyclic voltammetry curves of as-prepared QAU-1-M samples at 20, 30, 40, 50 and 60 mV s^{-1}.

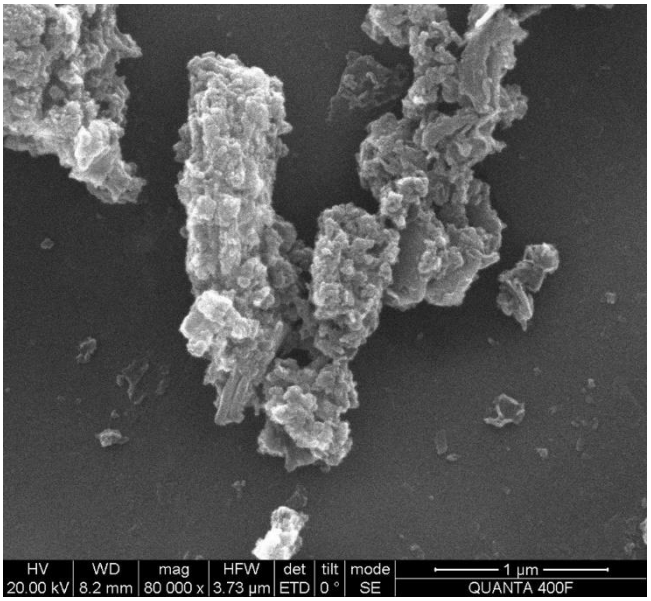

Figure S15. SEM image of QAU-1-FeNi(1:2) after OER measurements.

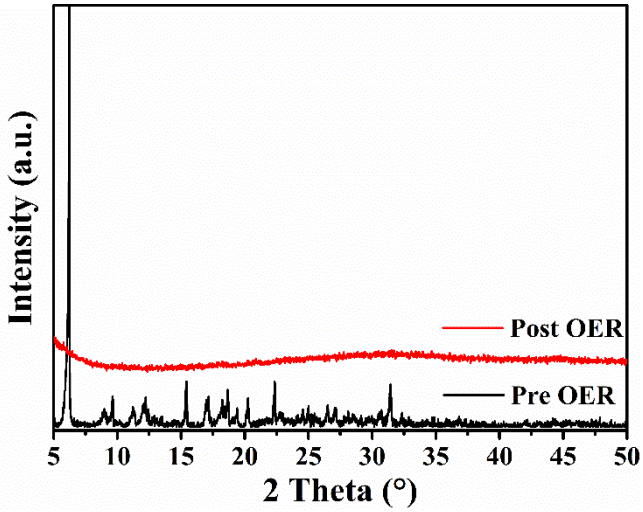

Figure S16. The XRD patterns of QAU-1-FeNi(1:2) before and after OER.

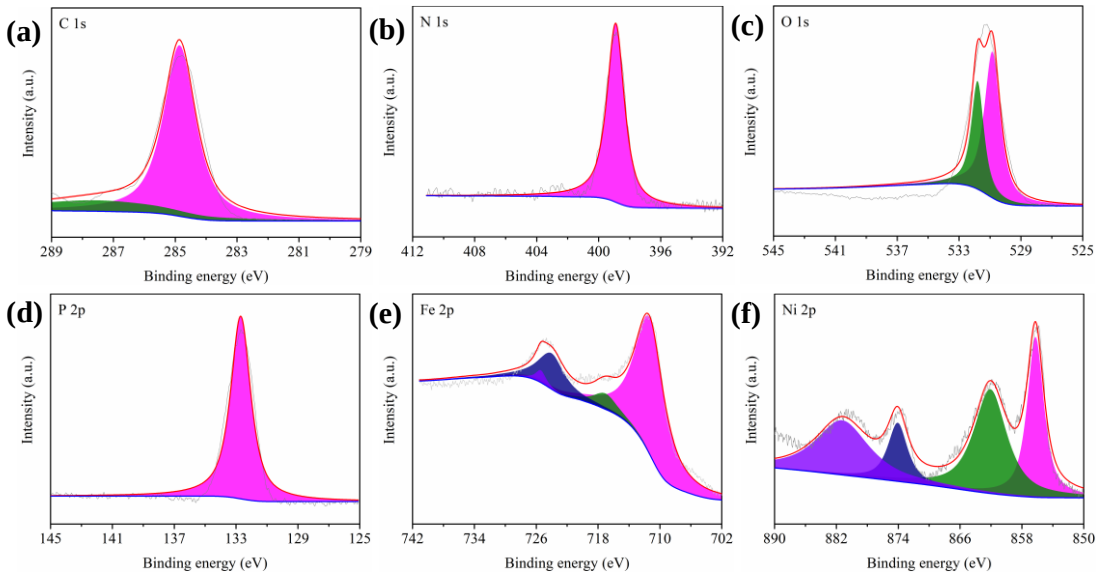

Figure S17. XPS survey spectra of QAU-1-FeNi(1:2) after OER.

REFERENCES

[1] M. Taddei, F. Costantino, F. Marmottini, A. Comotti, P. Sozzani, R. Vivani, *Chem. Commun*. 2014, **50**, 14831-14834.

[2] SAINT, Version 6.45; Bruker Analytical X-ray Systems Inc.: 2003.

[3] G. M. Sheldrick. SADABS, Version 2.10; Bruker AXS Inc.: Madison, WI, 2003.

[4] G. M. Sheldrick. SHELXS-97, Program for Crystal Structure Solution and Refinement; University of Göttingen, 1997.

[5] G. M. Sheldrick. SHELXL 2013 (Univ. Göttingen, 2013).

[6] P. Salcedo-Abraira, S. M. F. Vilela, A. A. Babaryk, M. Cabrero-Antonino, P. Gregorio, F. Salles, S. Navalón, H. García, P. Horcajada. Nickel phosphonate MOF as efficient water splitting photocatalyst. *Nano Res.* 2020, **14**, 450-457.

[7] B. Liu, Y. Xu, S.S. Bao, X.D. Huang, M. Liu, L.M. Zheng, *Inorg. Chem.* 2016, **55**, 9521-9523.

[8] R. Zhang, P.A. Russo, A.G. Buzanich, T. Jeon, N. Pinna, *Adv. Funct. Mater.* 2017, **27**, 1703158.

[9] P. Bhanja, Y. Kim, K. Kani, B. Paul, T. Debnath, J. Lin, A. Bhaumik, Y. Yamauchi, *Chem. Eng. J.* 2020, **396**, 125245.

[10] W. Xu, L. Feng, Z. Wang, B. Liu, X. Li, Y. Chen, *J. Electroanal. Chem.* 2020, **879**, 114786.

[11] P. Bhanja, Y. Kim, B. Paul, Y.V. Kaneti, A.A. Alothman, A. Bhaumik, Y. Yamauchi, *Chem. Eng. J*. 2021, **405**, 126803.

[12] M. Pramanik, C. Li, M. Imura, V. Malgras, Y.M. Kang, Y. Yamauchi, *Small*, 2016 **12**, 1709-1715.

[13] P. Feng, X. Cheng, J. Li, X. Luo, *Chem. Select*, 2018, **3**, 760-764.

[14] T. Zhou, Y. Du, D. Wang, S. Yin, W. Tu, Z. Chen, A. Borgna, R. Xu, *ACS Catal.* 2017, **7**, 6000-6007.

[15] T. Zhou, D. Wang, S. Chun-Kiat Goh, J. Hong, J. Han, J. Mao, R. Xu, *Energy Environ. Sci.* 2015, **8**, 526-534.

[16] Y.P. Liu, S.X. Guo, A.M. Bond, J. Zhang, S.w. Du, *Electrochim. Acta*, 2013, **101**, 201-208.

[17] W. X. Lu, B. Wang, W. J. Chen, J. L. Xie, Z. Q. Huang, W. Jin, J. L. Song, *ACS Sustainable Chem. Eng.* 2019, **7**, 3083-3091.